The Digital Twin of a New and Standardized Fullband Ear Simulator

Lars Birger Nielsen[1], Mads Herring Jensen[2]

[1] *Hottinger Brüel & Kjær A/S, 2830 Virum, Denmark, E-Mail: LarsBirger.Nielsen@hbkworld.com*
[2] *COMSOL A/S, 2800 Kongens Lyngby, Denmark, E-Mail: Mads.Jensen@comsol.dk*

Abstract

The use of virtual models designed to accurately reflect a physical object has over the last decade enabled an unprecedented precision in the simulation of the acoustical properties of devices before they materialize.

This paper introduces a new and standardized fullband ear simulator and explains some of the important characteristics, such as the acoustic impedance and the geometry of the ear simulator [1].

A corresponding virtual model – or digital twin – and the basis for the digital twin is explained.

For the physical fullband ear simulator and its digital twin the acoustical impedance is analysed to determine the correlation between the two.

Introduction

This paper presents the work of creating a new fullband virtual model or a digital twin of the new Type 4.3 Ear Simulator as specified in ITU-T P.57 [2]. The new fullband virtual model that is created is based on information that is available in the public domain [2]. A significant part of the work was dedicated to the task of establishing an ear drum impedance that would result in a transfer impedance as specified by the ITU-T P.57 standard.

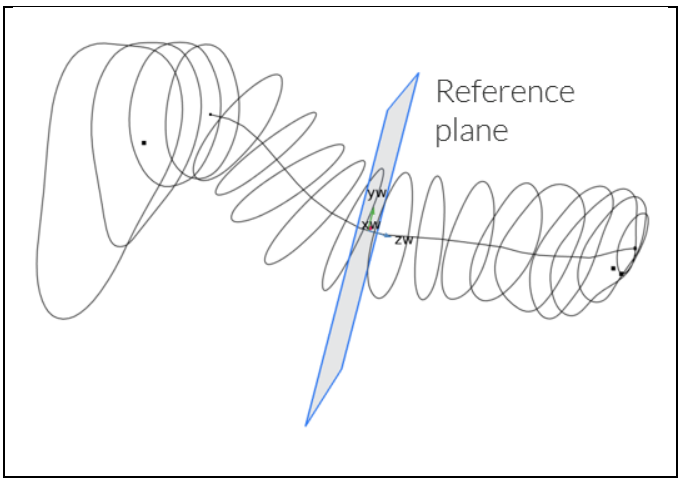

Figure 1: Cross-section areas that describes the average adult human ear canal geometry that are defined for the Type 4.3 Ear Simulator. The reference plan for determining the acoustic impedance is illustrated. More information is available in ITU-T P.57 [2].

Creating an initial virtual model

The geometry used by the model was constructed from the geometry description that is available in the ITU-T P.57 standard. A center line together with numerous cross-section areas are used to describe the ear canal. A reference plan for determining the acoustic impedance is defined and illustrated by the grey area in figure 1. When all the cross sections have been setup they are combined to a solid geometry, using the Loft operation in COMSOL Multiphysics [8].

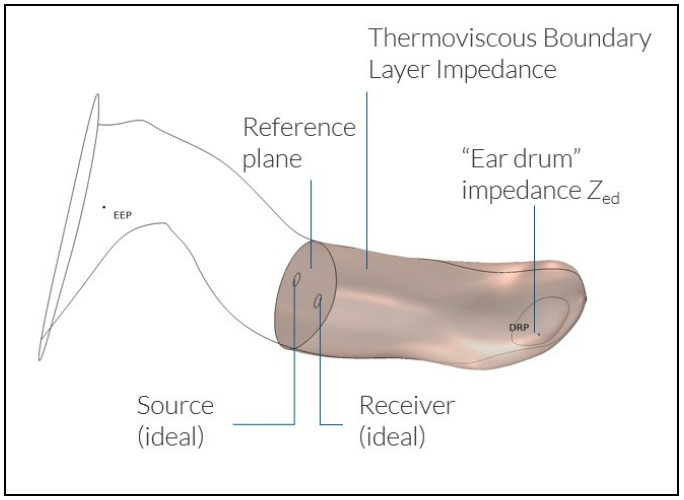

Figure 2: The virtual model of the ear canal. The model holds the ear drum impedance, the sound source, the receiver and the surface with a thermoviscous boundary layer.

The generated CAD geometry that is used for determining the optimized transfer impedance is the brown part of the geometry shown in figure 2. In figure 2 an ideal source, an ideal receiver, and an ear drum impedance as well as a thermoviscous boundary impedance condition is shown. These elements constitute the initial virtual model. Figure 3 holds an illustration of the computational mesh that is used by the virtual model.

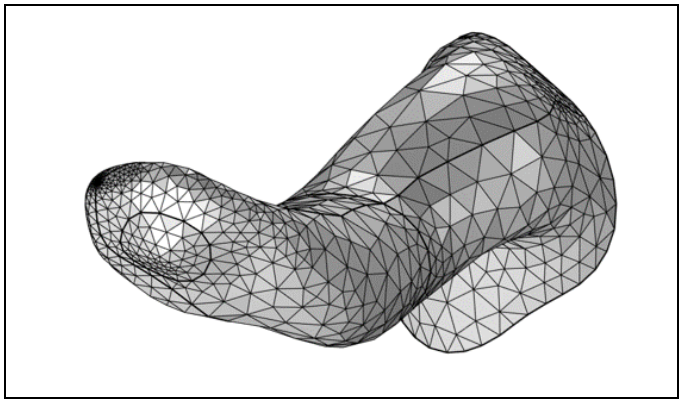

Figure 3: The computational mesh of the entire ear canal that are used by the virtual model.

To determine an ear drum impedance that will fulfil the transfer impedance specified by ITU-T P.57 it is required to provide an initial guess on an ear drum impedance. In the

work described in this paper the ear drum impedance model by Hudde and Engel [5], [6] and [7] was used as the initial guess. This seems very convenient as this model is already available in COMSOL Multiphysics. It should be noted that this model is valid in a reduced frequency range compared to the fullband frequency range from 20Hz to 20kHz. The reason being that it was never developed for the fullband frequency range.

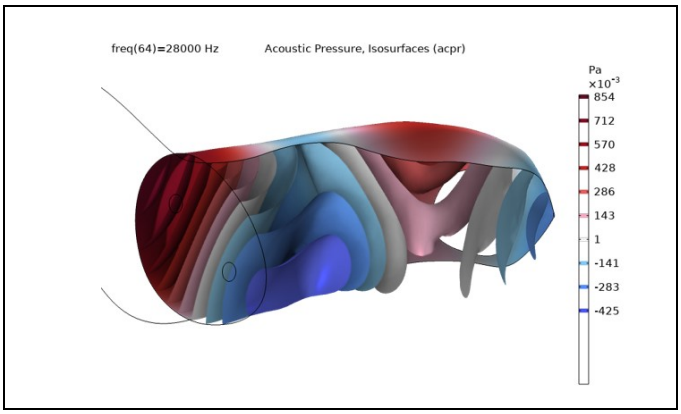

Figure 4: An example of the pressure isosurfaces at 28 kHz in the new fullband virtual model. This illustrates that at high frequencies a more complex wave fields than the just a plain waves propagation is present.

The impedance characteristics of the ear drum impedance model by Hudde and Engel are shown in figure 5. The resulting transfer impedance of the simulation, where this ear drum impedance has been applied are shown in figure 6. It should be noted that there is some agreement between the simulated transfer impedance and the transfer impedance specified by the ITU-T P.57 standard. It can also be observed that at higher frequencies there is a larger discrepancy between the two. This is to be expected, since the ear drum impedance by Hudde and Engel in to be used in a reduced frequency range compared to the fullband frequency range from 20Hz to 20kHz. The resulting input impedance are shown in figure 7.

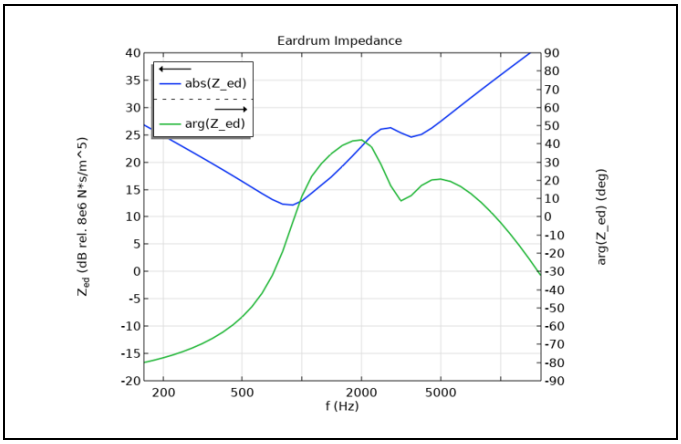

Figure 5: The magnitude response and phase response of a human eardrum impedance as presented in the studies conducted by Hudde and Engel.

A new fullband virtual model

Based on the initial virtual model that has been created, a more accurate model can be determined. This is accomplished by modifying the magnitude and phase of the impedance values at the ear drum in such a way that the deviation between the simulated transfer impedance and the standardized transfer impedance is minimized (the L2 norm is used at every frequency).

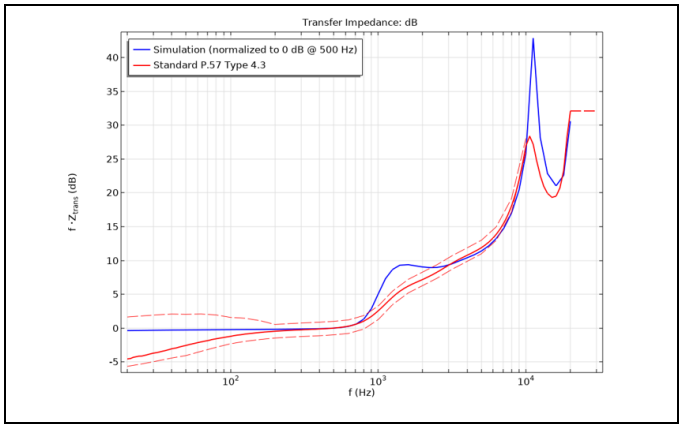

Figure 6: The result of the simulation when using the initial virtual model. The transfer impedance of the Type 4.3 Ear Simulator as it is defined by ITU-T P.57 (red curve) and the associated tolerances (dotted red curves). The corresponding transfer impedance of the human eardrum impedance as described by Hudde and Engel (blue curve).

In COMSOL Multiphysics this is done by using gradient based optimization and the control function feature, which controls the deviation from the initial guess at each frequency.

The result of this optimisation procedure is shown in figure 8. The Ear drum impedance of the new fullband virtual model is shown in red, the magnitude as a solid line and the phase as a dotted line.

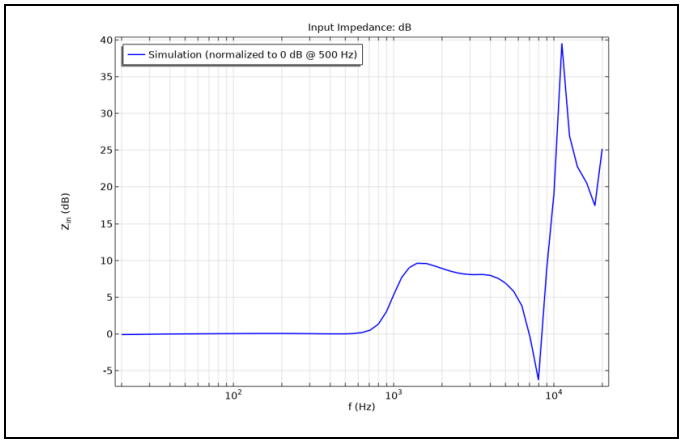

Figure 7: The input impedance of the human eardrum impedance as described by Hudde and Engel.

The ear drum impedance by Hudde and Engel is shown in blue, the magnitude as a solid line and the phase as a dotted line.

For easy comparison the transfer impedance of the initial virtual model (dotted black curve), the new fullband virtual model (blue curve) and the Type 4.3 Ear Simulator specified in ITU-T P.57 (red curve) can be seen in figure 9.

It can be observed that the new fullband virtual model has a few and minor deviations from the transfer impedance of the Type 4.3 Ear Simulator specified in ITU-T P.57. These can be reduced giving the control function more freedom in the optimization.

Comparison of Type 3.3 and Type 4.3

With the new fullband virtual model being established, a comparison of the impedance characteristics of the Type 3.3 Ear Simulator and the new Type 4.3 Ear Simulator can now easily be made. In this comparison the transfer impedance and the input impedance are investigated. It should be noted that the transfer impedance is now calculated between the DRP (Drum Reference Point) and the EEP (Ear Entrance Point).

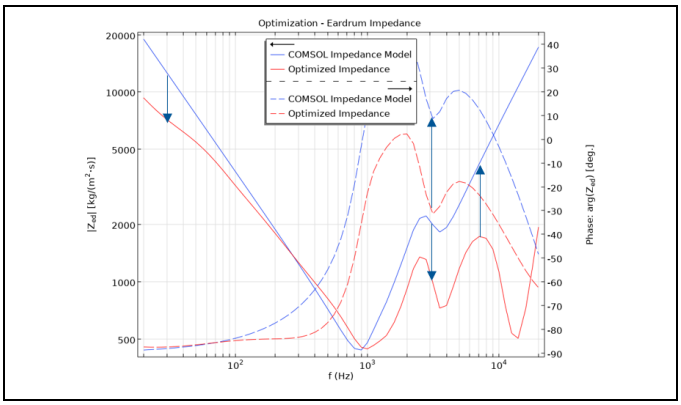

Figure 8: The magnitude response (blue curve) and phase response (dotted blue curve) of a human eardrum impedance as presented in the studies conducted by Hudde and Engel. This impedance forms the starting point for the optimization. The magnitude response (red curve) and phase response (dotted red curve) of a human eardrum impedance which complies with the transfer impedance defined by ITU-T P.57 Type 4.3 Ear Simulator.

For the simulation of the Type 3.3 Ear Simulator a 10 mm cylinder is added to the reference plan of the 711-coupler [4]. Figure 10 shows the pressure distribution of the Type 3.3 Ear Simulator at 10 kHz. Figure 11 shows the pressure distribution of the Type 4.3 Ear Simulator at 10 kHz.

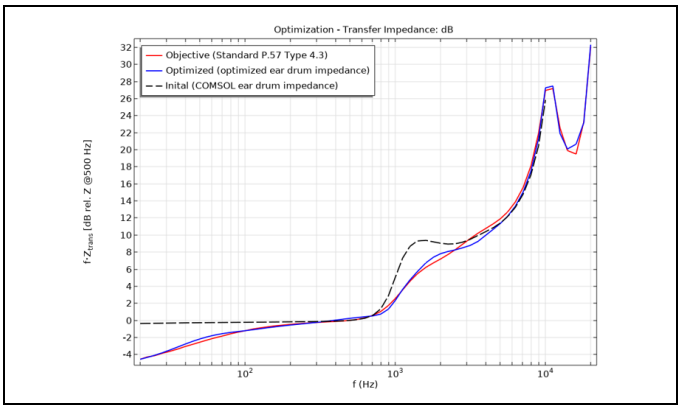

Figure 9: The magnitude of the transfer impedance of the virtual model of the Type 4.3 Ear Simulator (blue curve), the Type 4.3 Ear Simulator as defined by ITU-T P.57 (red curve), and the human eardrum impedance as presented in the studies conducted by Hudde and Engel (dotted black curve).

If an in-ear device is inserted very far into the ear, then in the physical Type 3.3 Ear Simulator there is a risk of blocking the slits that connects to the side volumes in the 711-coupler. These slits are necessary to provide the impedance specified by the standard, hence the loading of the in-ear device will be different than required.

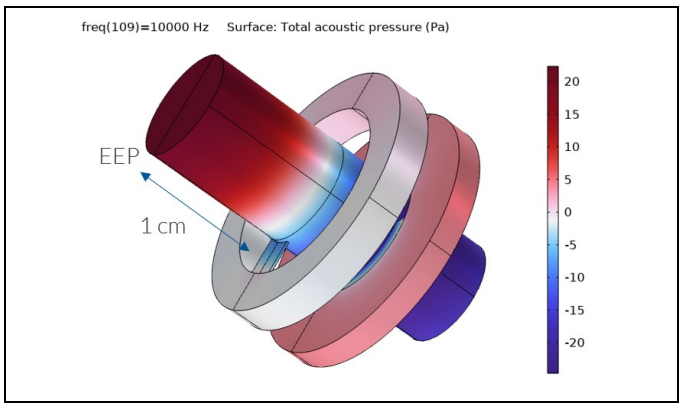

Figure 10: The figure shows the pressure distribution in the Type 3.3 Ear Simulator at 10kHz. The cylindrical shaped ear canal and the cavities of the 711-coupler can easily be recognised. It should be noted that for earphones that are intended to be inserted deep in the ear canal, it is likely that the slits connecting the cavities will be blocked, hence the acoustical load of the earphone would be different than intended by the design of the 711-coupler

For the physical Type 4.3 Ear Simulator inserting in-ear device very deep into the ear, the impedance specified by the standard is maintained, since the impedance is added at the ear drum.

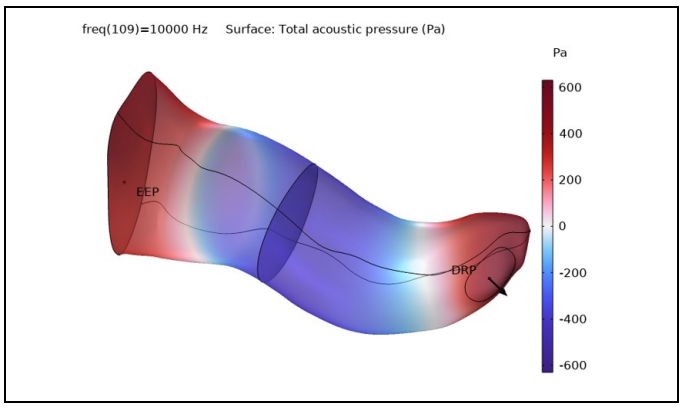

Figure 11: The figure shows the pressure distribution in the Type 4.3 Ear Simulator at 10kHz. The human shaped ear canal can easily be recognised. It should be noted that for earphones that are intended to be inserted deep in the ear canal, the acoustical load of the earphone would still be as intended by the design of the Type 4.3 coupler, because the load is presented at plan holding the DRP (Drum Reference Point).

The graph in figure 12 displays the simulated transfer impedance of the Type 3.3 Ear Simulator (green curve) and

the simulated transfer impedance of the Type 4.3 Ear Simulator (blue curve). It can be observed that in the lower frequency range there is a relatively good agreement between the two Ear Simulators. However, a characteristic roll-off at frequencies below 400Hz can be noted for the Type 4.3 Ear Simulator whereas for the Type 3.3 Ear Simulator is flat. At higher frequencies, a significant difference in the transfer impedance between the two can be observed.

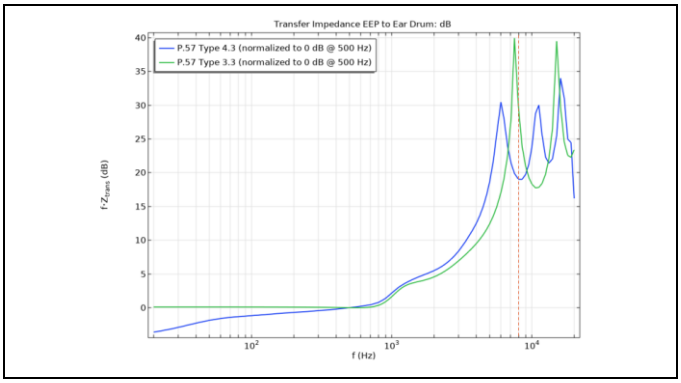

Figure 12: The magnitude of the transfer impedance determined between the EEP (Ear Entrance Point) and the DRP (Drum Reference Point). The graph shows the impedance of the virtual model of the Type 4.3 Ear Simulator (blue curve), and the impedance of the Type 3.3 Ear Simulator as defined by ITU-T P.57 (green curve). The dotted red line at 8kHz marks the frequency up to which the 711-coupler is specified.

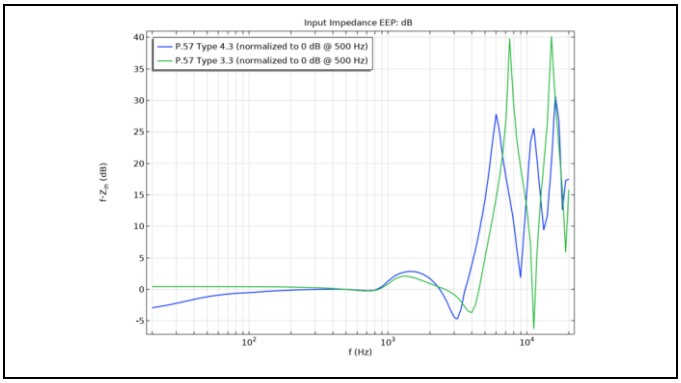

Figure 13: The magnitude of the input impedance determined at the EEP (Ear Entrance Point). The graph shows the impedance of the fullband virtual model of the Type 4.3 Ear Simulator (blue curve), and the impedance of the Type 3.3 Ear Simulator (green curve).

Conclusion

A new fullband virtual model of the Type 4.3 Ear Simulator specified by the ITU-T P.57 has been established. An ear canal geometry was created by utilizing the information provided about the Type 4.3 Ear Simulator in the ITU-T P.57 standard. Further to this an existing ear drum impedance model was modified to fit the transfer impedance also provide in the ITU-T P.57 standard, hence revealing a new fullband ear drum impedance model. This model has a more representative geometry of an average adult ear canal as well as an impedance that at higher frequency are more representative to that of an average adult human ear drum.

It should be noted that by utilizing an existing ear drum model that is known to be a viable representation of an average human ear drum impedance it is also more likely that the modified ear drum impedance will have some of the same human characteristics. If a somewhat random impedance where to be used the characteristics of the resulting impedance might lack important human impedance characteristics.

A future work item could be to further improve the fit of the new fullband virtual model with the Type 4.3 Ear Simulator specified by the ITU-T P.57. It is expected that this could be accomplished by increasing the resolution in the frequency domain. Likewise, a validation of a virtual device against a physical device, by performing simple measurement in the new fullband Type 4.3 Ear Simulator.

Figure 14: A commercially available physical realization of the Type 4.3 Ear Simulator according to ITU-T P.57.

References

[1] L. Nielsen. Evolution of human hearing simulation. DAGA 2021 Proceedings, pp. 75-78. 2021

[2] ITU-T Recommendation P.57: Artificial Ears. 2021

[3] ITU-T Recommendation P.58: Head and torso simulator for telephonometry. 2021

[4] IEC 60318-4 Ed. 1.0: Simulators of human head and ear Part 4: Occluded-ear simulator. 2010.

[5] H. Hudde & A. Engel, “Measuring and modelling basic properties of the human middle ear and ear canal. Part I: Model structure and measure techniques”, ACOUSTICA acta acoustica, vol.84, pp. 720–738 (1998).

[6] H. Hudde & A. Engel, “Measuring and modelling basic properties of the human middle ear and ear canal. Part II: Ear canal, middle ear cavities, eardrum, and ossicles”, ACOUSTICA acta acoustica, vol 84, pp. 894–913 (1998).

[7] H. Hudde & A. Engel, “Measuring and modelling basic properties of the human middle ear and ear canal. Part III: Eardrum impedances, transfer functions and model calculations”, ACOUSTICA acta acoustica, vol. 84, pp. 1091–1109 (1998).

[8] COMSOL Multiphysics, Version 6.0, including the Acoustics Module, the Optimization Module, and the Design Module, 2021.